Published in final edited form as:

Annu Rev Microbiol. 2013 ; 67: 21–42. doi:10.1146/annurev-micro-092412-155609.

3′ Cap-Independent Translation Enhancers of Plant Viruses

Anne E. Simon[1] and **W. Allen Miller**[2]

Anne E. Simon: simona@umd.edu; W. Allen Miller: wamiller@iastate.edu

[1]Department of Cell Biology and Molecular Genetics, University of Maryland, College Park, Maryland 20742

[2]Department of Plant Pathology and Microbiology, Iowa State University, Ames, Iowa 50011

Abstract

In the absence of a 5′ cap, plant positive-strand RNA viruses have evolved a number of different elements in their 3′ untranslated region (UTR) to attract initiation factors and/or ribosomes to their templates. These 3′ cap-independent translational enhancers (3′ CITEs) take different forms, such as I-shaped, Y-shaped, T-shaped, or pseudoknotted structures, or radiate multiple helices from a central hub. Common features of most 3′ CITEs include the ability to bind a component of the translation initiation factor eIF4F complex and to engage in an RNA-RNA kissing-loop interaction with a hairpin loop located at the 5′ end of the RNA. The two T-shaped structures can bind to ribosomes and ribosomal subunits, with one structure also able to engage in a simultaneous long-distance RNA-RNA interaction. Several of these 3′ CITEs are interchangeable and there is evidence that natural recombination allows exchange of modular CITE units, which may overcome genetic resistance or extend the virus's host range.

Keywords

noncanonical translation; eIF4E/eIF4G; 3′ UTR translation elements; RNA structure and function; internal ribosome-binding structures; long-distance RNA-RNA interactions

INTRODUCTION

In the past twenty years, it has become increasingly apparent that the 3′ untranslated region (UTR) of an mRNA is a hub for posttranscriptional control of gene expression, including translation. This is clearly evident for positive-strand RNA viruses (40, 53), the most successful and abundant type of virus infecting eukaryotes (33). In addition to serving as mRNAs for translation of virus-encoded products, the genomes of positive-strand viruses have the complication that they serve as templates for replication, a process entirely different from and antagonistic to translation. At an early stage of infection, when only one or a few viral genomes are present in a cell, these viral RNAs must gain a foothold and compete with host messages for the translational machinery. Many plant viruses have

DISCLOSURE STATEMENT

The authors are not aware of any affiliations, memberships, funding, or financial holdings that might be perceived as affecting the objectivity of this review.

evolved sequences and structures in their 3′ UTRs that allow the viral genome to not only undergo translation and replication, but also facilitate a switch between these two mutually incompatible processes necessary for maintaining a successful infection (7, 33, 70).

Eukaryotic cellular mRNAs contain a 5′ cap structure consisting of a 7-methyl GTP attached in a 5′-5′ linkage to the 5′ terminal nucleotide of the mRNA. This arrangement is required for recognition by translation initiation factor eIF4E, which contains a cap-binding pocket that specifically recognizes 7-methyl GTP with 100-fold-higher affinity than GTP (36). eIF4E partners with the multifunctional scaffolding protein eIF4G to form the eIF4F complex (41). eIF4G also interacts with eIF4B, the helicase eIF4A, and poly(A)-binding protein (PABP), which when also bound to the poly(A) tail causes circularization of the mRNA. eIF3 brings the 43S ribosomal preinitiation complex to the eIF4G scaffold, after which scanning toward the initiation codon commences (18). In addition to domains for binding the above factors, eIF4G contains three RNA-binding domains and the MIF4G domain, which is essential for ribosome scanning (26, 43). After encountering an initiation codon in a proper context, eIF5B mediates the joining of the 60S subunit to form the 80S ribosome and the initiation factors are released as translation elongation commences (18).

Most plant positive-strand RNA viruses do not have a cap structure (e.g., m7GpppN) at the 5′ end of their genome and thus must recruit either eIF4F or the ribosome directly by noncanonical means to translate efficiently. These RNA genomes may contain a 5′ genome-linked protein (VPg) as in the *Secoviridae*, *Potyviridae*, and the sobemo-like viruses, or the genome may simply terminate with a free 5′ phosphate. Many, if not all, plant viruses in the latter group contain cap-independent translation enhancers (CITEs) in their 3′ UTRs (7, 23, 33), with the elements sometimes including upstream coding sequences (3). 3′ CITEs can functionally substitute for the 5′ cap structure with high efficiency, leading to ribosome entry at or near the 5′ terminus followed by ribosome scanning to the initiation codon (8, 33, 44). Although these 3′ CITEs facilitate cap-independent translation, usually they do not function like the better known internal ribosome entry sites (IRESs), which are associated with viral RNAs that infect many mammals and insects (46). Currently, most 3′ CITEs have been delineated in genomes of viruses within the large family *Tombusviridae* (eight genera); in the closely related *Luteovirus* genus of the family *Luteoviridae*; or in the genus *Umbravirus*, which are viruses without coat proteins that have not been assigned to a family. This review focuses on recent advances in our understanding of the structures of these 3′ CITEs, how they recruit the translational machinery, and how they communicate with the 5′ end of the viral genome. These studies have not only provided information about a crucial step in the life cycle of many viruses, but have also illuminated alternative ways that mRNAs can recruit translation factors and ribosomes.

3′ CITEs IN THE *TOMBUSVIRIDAE* AND *TOMBUSVIRIDAE*-RELATED VIRUSES

Translation Enhancer Domain

The first 3′ CITE discovered was the translation enhancer domain (TED) of *Satellite tobacco necrosis virus* (STNV), a subviral RNA (1.2 kb) with a single open reading frame

(ORF) that encodes its capsid protein. Two reports described a 120-nucleotide sequence (TED) near the 5′ end of the 3′ UTR that is capable of functionally replacing a 5′ cap (4, 56) (Figure 1). Deleting the TED reduces translation at least 20-fold and adding a 5′ cap, but not a poly(A) tail, restores translation. The TED binds to eIF4F with high affinity (11), is predicted to form a long stem loop with several bulges of six to eight bases, and has no strong uninterrupted helices (59). Because this structure has not been confirmed experimentally, the features that make it attractive to eIF4F remain unknown. The apical loop of the STNV TED contains a sequence that is complementary to the apical loop of a 5′ terminal hairpin, suggesting the formation of a long-distance, kissing-loop interaction (Figure 1). Two carmoviruses [*Pelargonium line pattern virus* (PLPV) and *Pelargonium chlorotic ring pattern virus* (PCLPV)] contain a similar TED-like structure within their 3′ UTRs and both have a sequence in their apical loops that can putatively form a kissing-loop interaction with a 5′ proximal hairpin (Figure 1). The core of the PLPV/PCLPV interacting sequence (YGCCA; Y is a pyrimidine) is conserved in other carmovirus 3′ CITEs that engage (or are predicted to engage) in similar long-distance interactions with 5′ proximal sequences (3) (Table 1). The STNV TED RNA-RNA interaction has not been confirmed, as mutating the terminal loop sequence reduced translation only modestly, and reestablishing potential base-pairing by mutating the 5′ UTR did not restore full translation (29). However, artificial constructs that do not contain STNV coding sequences were used in this study, and it is possible that additional sequences are necessary in vivo to support the formation or function of the kissing-loop interaction. Altogether, these observations suggest that TED participation in long-distance interactions is needed for optimal infectivity.

Barley yellow dwarf virus–Like Element

One of the best-characterized 3′ CITEs is the *Barley yellow dwarf virus*-like element (BTE) (14, 63) (Figure 2), which is present in all members of the *Luteovirus*, *Dianthovirus*, and *Necrovirus* genera and in some umbraviruses (30, 31, 52, 62, 64). The BTE is distinguished by the presence of a 17-nucleotide conserved sequence: GGAUCCUGGgAaACAGG (62), with the underlined bases pairing to form a small stem loop, designated SL-I (13, 64). The bases in lower case can vary, but the 5-nucleotide terminal loop always fits the consensus of a GNRNA pentaloop (N is any base, R is a purine) first identified in λ *boxB* RNA (25). Like the well-characterized GNRA tetraloop (16), the G and A at the base of the loop form a propeller-twisted base pair with the remaining bases (except for the fourth base of the pentaloop) stacked in a helical alignment with the adjoining stem, adding substantial stability to the structure (25). The fourth base of the GNRNA protrudes into the solvent, making it potentially accessible for interactions with protein (25). Whether SL-I of the BTE actually forms this particular structure has yet to be shown, but given that it fits the consensus, such a structure is likely.

The BTE, including the 17-nucleotide conserved sequence, forms a series of stem loops radiating from a central hub (64) (Figure 2). Together with the helix that connects the BTE to the rest of the viral genome, the *Barley yellow dwarf virus* (BYDV) BTE has four helices (13); the necrovirus BTE has three helices; and the dianthovirus BTE has six helices, giving it a two-dimensional asterisk-like structure (64). At the hub of the helices are unpaired bases (i.e., not engaged in any apparent Watson-Crick base pairing) that also play a critical role in

function. Mutating almost any base in the hub greatly reduces activity of the BYDV BTE (13, 24), suggesting that there are critical non-Watson-Crick interactions that are not simple to predict around the helical junctions. Removal of SL-II from the BYDV BTE, making the two-dimensional structure more similar to a necrovirus BTE, rendered the BTE inactive (13).

Other viruses have unusual BTE variants. The BTEs of *Rose spring dwarf-associated luteovirus* and two umbraviruses have many more unpaired bases around the central hub than those shown in Figure 2. In addition, the BTE of *Groundnut rosette umbravirus* has major deviations from the 17-nucleotide conserved sequence. These deviations from consensus may explain why these three BTEs are weaker translational enhancers than those that fit the consensus more closely (64).

The BTE binds eIF4G with unusually high affinity, which is sufficient to facilitate translation in the absence of eIF4E (57). eIF4E alone has no stimulatory effect, whereas eIF4G and eIF4E together (i.e., eIF4F) stimulate translation to levels that are 20% to 30% greater than eIF4G alone. Truncated eIF4G lacking the eIF4E- and PABP-binding sites stimulates translation as efficiently as full-length eIF4G (24, 57). Footprinting experiments revealed that eIF4G protects SL-I, which is within the 17-nucleotide conserved sequence, as well as additional bases around the hub (Figure 2). Addition of eIF4E enhanced the level of protection (24), consistent with binding constants for eIF4G (177 nM) and eIF4F (37 nM) (57). The authors proposed that SL-I interaction with eIF4F resembles *boxB* RNA of bacteriophage λ (which contains a well-characterized GNRNA pentaloop) interacting with λ protein N and host protein NusA. NMR of *boxB* in the presence of a fragment of the N protein and NusA revealed specific interactions between an arginine-rich region and the 5-bp *boxB* helix, with a tryptophan residue base-stacking on the helically arranged bases of the GNRNA pentaloop. This binding allows the *boxB*-bound N protein and the protruding fourth base of the GNRNA loop to interact with the NusA protein. Kraft et al. (24) proposed that a similar interaction may recruit eIF4G to the BTE SL-I, with the fourth base of the GNRNA loop enhancing binding of eIF4E [which does not bind in the absence of eIF4G (57)]. However, additional interactions around the helical junction are also necessary, as SL-I alone or with its flanking bases is insufficient to facilitate cap-independent translation.

A stable hairpin outside the 17-nucleotide conserved sequence in all BTEs contains an apical loop sequence complementary to a sequence in the 5′ UTR (64) (Table 1). A long-distance RNA-RNA interaction between these viral sequences is required for efficient translation by the BYDV BTE but can be replaced by nonviral sequences outside the BTE (44). The sole exception is the BTE of *Red clover necrotic mosaic virus* (RCNMV), as mutating several loops with sequences complementary to the 5′ UTR had no significant effect on translation (49). However, the loops were not mutated simultaneously, leaving open the possibility that redundant long-distance interactions exist. Alternatively, as discussed for the STNV TED, base-pairing may be biologically relevant but not crucial for the constructs and assays used. Base-pairing between the BTE and 5′ UTR led to a model in which eIF4F binds the BTE without obscuring the loop complementary to the 5′ UTR. However, available data do not distinguish between (*a*) the 40S subunit binding the eIF4F-BTE complex before the BTE base-pairs with the 5′ end, followed by delivery to the 5′ terminus, and (*b*) delivery of the

bound translation factors to the 5′ end after which 40S is recruited. This is a crucial question that requires answers for all 3′ CITEs.

Panicum mosaic virus-Like Translational Enhancer

Viruses in the *Panicovirus* genus, along with some carmoviruses and the umbravirus *Pea enation mosaic virus RNA 2* (PEMV2), contain a 3′ CITE termed the PTE (*Panicum mosaic virus*-like translational enhancer) based on its initial discovery in *Panicum mosaic virus* (PMV) (1). The PTE, unlike nearly all other known uncapped RNAs, binds eIF4E with high affinity (K_d = 58 nM), even in the absence of eIF4G (66). The only other natural RNA that binds eIF4E without 7-methylguanosine modification is the eIF4E-sensitive element (4E-SE) element of histone H4 mRNA (27).

The PTE consists of a three-way branched helix with a large G-rich bulge (G domain) in the main stem (66) (Figure 3). Connecting the two helical branches at the branch point is a short C-rich or pyrimidine-rich bulge (C domain). In the G domain, one guanylate is hypersensitive to SHAPE reagents that modify the 2′-hydroxyl of non-Watson-Crick base-paired nucleotides. In the presence of mutations in the C domain or in the absence of magnesium ions, this hypersensitivity is lost and the G residues in the G domain are equally modified as expected for a uniformly single-strand RNA (65). These findings led Wang et al. (65) to propose the existence of a pseudoknot between the G domain and the C domain. Many different mutations designed to reestablish disrupted base-pairing between these regions were ineffective at restoring cap-independent translation (66), suggesting that the primary sequence is important. Footprinting experiments indicated that the region around this pseudoknot is protected by eIF4E (65). This finding led to a model positing that pseudoknot interaction forces the SHAPE-hypermodified G residue to protrude from the PTE into the cap-binding pocket of eIF4E (Figure 3*b*). eIF4E binding is proposed to be strengthened by interactions of the rim of the cap-binding pocket with portions of the PTE around the pseudoknot. This would compensate for the absence of the 7-methyl group on the RNA. However, this model has not been tested.

The 5′ side hairpin of all PTEs, except for the PEMV2 PTE, has an apical loop that is complementary to the apical loop of a hairpin at or near the 5′ end of the viral RNA (3) (Figure 3*a*). In panicoviruses, the sequence complementary to the PTE is in the apical loop of a 5′ terminal hairpin, whereas in the carmovirus *Saguaro cactus virus* (SCV), the 5′ complementary sequence is in the loop of a coding region hairpin (3) (Table 1). The carmovirus PTE sequence that engages in the RNA-RNA interaction has the same conserved motif (YGCCA/UGGCR) found in carmovirus TED-like elements and I-shaped structure (ISS) elements (see below), with either sequence present at either end (Table 1). The 5′ interacting sequence in general is located in the apical loop of hairpins located either at the 5′ terminus or in the coding region within 150 nucleotides of the 5′ end of the mRNA. The conservation of interacting sequences suggests a function for the paired sequences beyond simple kissing-loop formation, but this function remains unknown.

I-Shaped Structure

3′ CITEs with a common I-shaped structure (ISS) have been found in carmoviruses and in *Maize necrotic streak virus* (MNeSV), a unique member of the *Tombusviridae* (50). The MNeSV ISS contains a key central domain with a four-base helix and flanking bulged sequences (Figure 4*a*). Mutagenesis and structure probing found significant roles for non-Watson-Crick interactions, and possibly alternative structures, as few mutations in the core region are tolerated, even when conserving the proposed secondary structure (34, 35). Translational enhancement by the MNeSV ISS in factor-depleted wheat germ extracts requires intact eIF4F, unlike the BTE for which eIF4G was sufficient. The MNeSV ISS also binds only to intact eIF4F (K_d = 190 nM), unlike the BTE (binds eIF4G) or the PTE (binds eIF4E). As with other 3′ CITEs, base-pairing between the terminal loop and its complementary sequence in a 5′ UTR hairpin is necessary for efficient translation. The long-distance interaction and eIF4F binding can occur simultaneously, supporting the hypothesis that the long-distance pairing delivers eIF4F to the 5′ end. Toeprinting assays were consistent with ribosome scanning from the 5′ end to the start codon, which required the 3′ CITE (34).

Direct involvement of the ISS of the carmovirus *Melon necrotic spot virus* (MNSV) and eIF4E was inferred genetically, because a single point mutation in eIF4E provides recessive resistance to MNSV in cucumber (*nsv* gene), including strain MNSV-M*a*5 (37). A resistance-breaking strain, MNSV-264, contains mutations in the central portion of the bulged stem loop in the ISS that are sufficient to break resistance (58). In wheat germ extracts, uncapped reporter constructs containing the cucumber *nsv* resistance-breaking MNSV-264 ISS in the 3′ UTR translated five times more efficiently than those containing the noninfectious MNSV-M*a*5 ISS. However, addition of eIF4E from cucumber susceptible to both viruses allowed the MNSV-M*a*5 ISS to translate nearly as efficiently as the construct containing the MNSV-264 ISS (58).

Moreover, the MNSV-M*a*5 reporter construct translated efficiently only in virus-susceptible melon protoplasts, whereas the MNSV-264 construct translated most efficiently in resistant protoplasts (58). Based on Mfold predictions, Nicholson et al. (34) proposed that the MNSV-M*a*5 ISS forms an inverted version of the ISS, with the 3′ and 5′ ends reversed, relative to the MNSV-264 ISS, MNeSV ISS, and other ISS. However, the inverted functional orientation does not conform well with the alternative ISS that these authors predicted on the basis of more recent in vivo evolution studies (34, 35) (Figure 4*a*). The ISS from either strain interacts with the MNSV 5′ UTR in a strain-independent fashion. The apical loop of the MNSV ISS contains the conserved carmovirus motif (Table 1), and its 5′ partner hairpin is in the 5′ coding sequence.

Y-Shaped Structure

The 3′ CITE of viruses within the genus *Tombusvirus* has a conserved Y-shaped structure (YSS) with three major helices that are all substantially longer than the three helices of the PTE (8, 9, 67) (Figure 4*b*). The 5′ side hairpin engages in a required long-distance kissing-loop interaction with a 5′ UTR hairpin loop. The base-pairing sequence (5′-GGUCG) shares only limited sequence similarity with the carmovirus consensus sequence. Mutations that

maintain the structure of the three stems in the YSS of *Tomato bushy stunt virus* (TBSV) do not have a substantial impact on translation, unlike alterations in junction residues between helices and in a large asymmetric bulge in the major supporting stem (9). Addition of translation factors to factor-depleted wheat germ extracts revealed that the YSS of *Carnation Italian ringspot virus* (CIRV) requires eIF4F or eIFiso4F for efficient translation (35). As with translation associated with all of these 3′ CITEs, the YSS facilitates ribosome scanning from the 5′ end.

T-Shaped Structure

3′ CITEs that assume a three-dimensional T-shaped structure (TSS) were first discovered in the carmovirus *Turnip crinkle virus* (TCV) (28). Although all carmoviruses share similar 3′ end structural organization [stable 3′ terminal hairpin and an upstream hairpin with a large internal symmetrical loop (H5) that is linked to the 3′ terminus through a pseudoknot] (73), carmoviruses have a surprising variety of CITEs immediately upstream of the conserved 3′ terminal structures (3, 38, 54). TCV and the related carmovirus *Cardamine chlorotic fleck virus* (CCFV) contain a unique set of three hairpins (including H5) and two pseudoknots that fold into a TSS that is topologically similar to a tRNA, as predicted by molecular modeling and confirmed by small-angle X-ray scattering (SAXS) and NMR (28, 74) (Figure 5*a*). Unlike the Tymo, Rubi, and Tobamo lineages of Supergroup 3 viruses that have 5′ caps and 3′ terminal, aminoacylated tRNA-like structures (6, 7), TCV and CCFV lack 5′ caps and the 3′ TSS are present in an internal location, precluding aminoacylation. The TCV TSS binds to yeast and *Arabidopsis* 80S ribosomes and 60S subunits, and binding is important for CITE activity (54). The TCV TSS competes for 80S ribosome binding with a P-site-binding tRNA, and recent cryo-electron microscopy of 80S ribosomes bound to the TSS places the TSS in the P site, interacting with peptidyltransferase center helices H89/H90, helices H69 and H95 of 25S rRNA, and proteins L10 and L11 of the 60S subunit (J. Pallesen & J. Frank, unpublished data). The P-site proximal placement was confirmed by high-throughput SHAPE (hSHAPE) structure mapping of in situ ribosomal RNAs, which reports on residues with altered flexibility in the presence of the TCV TSS (J. Leschine, J. Dinman & A.E. Simon, unpublished data).

For the TSS to function as a 3′ CITE, additional elements are required, including an adjacent A-rich repeat, the terminal and internal loops of upstream hairpin H4, and portions of a largely unstructured region upstream of H4 (54). The A-rich repeat is currently thought to interact with the adjacent downstream pseudoknot Ψ_3, as disruption of either the A-rich region or Ψ_3 enhances flexibility in the residues of the other's structure, as assayed by in-line RNA structure probing (70).

All these TCV 3′ UTR elements, together with additional coding region sequences, form an integrative network of noncanonical interactions that are important for virus accumulation (71, 72). In the presence of the RNA-dependent RNA polymerase (RdRp), this higher-order structure is substantially disrupted, including extensive alteration of the region of the TSS that mimics the tRNA acceptor arm (H4a/Ψ_3) (70). Because the tRNA acceptor arm and its TSS mimic are ribosome-binding sites (51, 54), it was proposed that the RdRp-mediated

conformational switch arrests 3′ ribosome binding and CITE function, thus allowing transcription to initiate at the 3′ end without ribosome-bound impediments (70).

Because TCV lacks a detectable RNA-RNA interaction that links sequences proximal to the 5′ and 3′ ends to circularize the genome (55), a key question is whether and how 60S subunits bound to the 3′ TSS are recruited to the 5′ end. The discovery of a 40S-binding site in the 5′ UTR of TCV led to the hypothesis that circularization of the template may result from the 40S bound to the 5′ end combining with 60S bound to the 3′ proximal TSS to form 80S ribosomes (55). In support of this hypothesis, structural probing of the TCV 5′ UTR in the presence of 80S ribosomes revealed substantive differences in nucleotide flexibility when the 3′ UTR of TCV was included in the reaction. These differences were interpreted to result from 80S ribosomes binding simultaneously to both 5′ and 3′ TCV sequences, which altered ribosome interaction with the 5′ end (55). While it is currently unknown whether additional translation factors interact with the TSS or the TSS-ribosome complex, translation of TCV constructs containing the genomic or subgenomic RNA 5′ UTR and 3′ UTR is reduced in *Arabidopsis* cells deficient in eIF4G (68, 69).

A second TSS with 3′ CITE activity was recently discovered in the central region of the 3′ UTR of PEMV2, 9 nucleotides upstream of the PTE 3′ CITE (Figure 5*b*,*c*). The kissing-loop TSS (kl-TSS) comprises a three-way branched structure with a 5′ side hairpin (3H1) that engages in a long-distance kissing-loop interaction with a coding sequence hairpin (Figure 3*a*) that uses the conserved carmovirus interacting motif (10) (Table 1). The kl-TSS differs from the TCV TSS in that it binds to 40S and 60S ribosomal subunits and to 80S ribosomes (10). The kl-TSS does not compete with the TCV TSS for 80S binding, suggesting a binding site outside the P-site (F. Gao & A.E. Simon, unpublished data). Ribosome binding is compatible with the long-distance interaction (F. Gao & A.E. Simon, unpublished data), suggesting that the binding site within the ribosome must allow for the presence of upstream and downstream viral sequences as well the interacting 5′ region hairpin. The orientation of the kl-TSS with respect to a tRNA is currently unknown, and two possible orientations are shown in Figure 5*b*,*c*. The downstream proximity of the PTE 3′ CITE suggests that the kl-TSS provides the missing bridge to the 5′ end in this unusual PTE. Alternatively, interaction of the nearby PTE bound to eIF4E may enhance ribosome binding to the kl-TSS. It is currently unknown why 3′ CITEs capable of sequestering ribosomes or ribosomal subunits exist in the 3′ UTR, but the most likely explanation is that TSS-type 3′ CITEs enhance the recycling of posttermination ribosomes, thereby increasing the rate of ribosome reinitiation at the 5′ end. The three-way branched organization of the kl-TSS is a common RNA structure, which could suggest that ribosome recognition of elements other than a 5′ cap (via initiation factors) or IRESs in coding RNAs may be more widespread than currently thought.

3′ CITEs IN OTHER VIRUSES

A 3′ CITE was discovered in viruses in the genus *Nepovirus*, which are unrelated to the other viruses discussed in this article. Nepoviruses belong to the order *Picornavirales* and contain a VPg at the 5′ end and a poly(A) tail. Karetnikov et al. (20, 22) identified sequences in the 3′ UTRs of RNAs 1 and 2 of *Blackcurrant reversion virus* that confer efficient cap-

independent translation. As with CITEs discussed above, the nepovirus 3′ CITE must base-pair with 5′ proximal sequences, which are located in the 5′ UTR in nepoviruses. Unlike other CITEs, placement of the 5′ UTR sequence between two ORFs in artificial constructs confers efficient translation of the second ORF if the 3′ CITE is present in the 3′ UTR (21, 22). Thus, the 3′ CITE together with its partner sequence upstream of the ORF serves as a split IRES. Pyrimidine-rich tracts in the 5′ UTR, which are predicted to base-pair to 18S rRNA, stimulate translation but are not essential (22). The secondary structure of the 3′ CITE has not been determined but is predicted to contain a pseudoknot (22).

While BYDV and other viruses of the genus *Luteovirus* contain a BTE, viruses of the *Polerovirus* and *Enamovirus* genera of the family *Luteoviridae* appear to lack a 3′ CITE (W.A. Miller, unpublished data). Instead, the VPg at the 5′ end of these viral genomes may facilitate translation via its interaction with translation initiation factors (45). The same may be true for the sobemoviruses, which are closely related to the poleroviruses. The VPg of the sobemovirus, *Rice yellow mottle virus*, interacts directly with eIFiso4G, and mutations in eIFiso4G that disrupt the interaction confer resistance, whereas compensating mutations in the VPg that restore the interaction also restore virus virulence (15). To our knowledge, no CITE has been reported for a sobemovirus.

MODULAR EVOLUTION OF 3′ CITEs

The 3′ UTRs of viruses in the *Tombusviridae* and their cousins have likely evolved different CITEs to provide alternative ways of binding tightly to the surface of eIF4F or its eIF4E and eIF4G subunits, akin to a SELEX reaction in which RNAs can be evolved in vitro to bind ligands with high affinity (12). Evolution of a 3′ CITE would have allowed these compact viral RNAs to compete with host mRNAs without the need for a 5′ cap (a genetic burden requiring an additional viral gene) and perhaps would have allowed them to bypass host translational control mechanisms that regulate cap binding by eIF4F. A remarkable feature of the distribution of 3′ CITEs among the *Tombusviridae* and *Tombusviridae*-like viruses is that it often does not correlate with taxonomy (Figure 6). Carmoviruses have at least four types of CITEs (TED-like, PTE, ISS, TSS), with additional classes remaining to be discovered (note the uncolored viruses in Figure 6). Some umbraviruses have BTEs or weakened versions of BTEs that may be nonfunctional relics, one umbravirus has a PTE and kl-TSS, and others have no recognizable CITE. Viruses in two different families (*Luteoviridae* and *Tombusviridae*) can harbor a BTE, whereas other viruses in those families have no BTEs. Thus, either CITEs are sufficiently simple that they have evolved independently many times and are the products of convergent evolution, or—more likely—these viruses regularly recombine and are able to function with different types of CITE.

In support of modular evolution of 3′ CITEs, some CITEs can be exchanged between viruses artificially with little or no deleterious effects on virus accumulation. Replacement of the YSS of tombusvirus CIRV with an ISS (34) or PTE (35) that is modified to contain the compatible, long-distance interacting sequence yields viral RNAs that translate more efficiently than in the absence of a 3′ CITE and that replicate efficiently in protoplasts. In contrast, replacing the same CIRV YSS with the *Tobacco necrosis virus*-D (TNV-D) BTE does not facilitate efficient translation and does not yield infectious virus (35). Remarkably,

the CIRV-ISS and CIRV-PTE chimeras replicate and spread in whole plants, with the latter producing a more aggressive infection in *Nicotiana benthamiana* compared with wild-type CIRV. In addition, progenies of the CIRV-ISS chimera become more virulent with multiple passages (35), and sequencing revealed base changes in the core of the ISS (35).

One advantage to the natural exchange of 3′ CITEs is their contribution to overcoming genetic resistance. In addition to chemical and physical barriers to the virus vector, plants restrict most viral infections by using multiple layers of active resistance that can lead to degradation of the virus by RNA silencing (61), restriction of virus replication (17), or limitation of movement by destroying cells surrounding the infection site (39). In contrast, passive (recessive) resistance (lack of factors required for virus infection) frequently involves incompatibility between viral translation elements and their cognate translation initiation factors (47, 60). Recessive resistance to potyviruses, which have a 5′ VPg, an IRES in the 5′ UTR, and 3′ poly(A) tails, has long been known to map to specific, incompatible eIF4E isoforms (48). These isoforms retain 5′ cap–binding activity but cannot engage in a required, but functionally undefined, direct interaction with the potyviral 5′ VPg (32, 42). Of the 14 known recessive resistance genes, 12 map to eIF4E or its functionally redundant isoform, eIFiso4E, with the remainder mapping to eIF4G or its isoform, eIFiso4G (60). As described above, resistance to MNSV maps to a particular eIF4E isoform that engages in a required interaction with its ISS 3′ CITE (58). *N. benthamiana*, which does not contain a compatible version of eIF4E, can be infected only by MNSV-264, the resistance-breaking strain (5). MNSV-264 is a natural recombinant, containing a segment from the 3′ CITE to the 3′ end that originated from a different, unknown carmovirus (38). This suggests that RNA recombination, which is prevalent among members of the *Tombusviridae* (2, 19), can lead to the acquisition of 3′ CITEs from heterologous viruses that do not require interaction with a particular host factor but that do maintain the critical RNA-RNA interaction through the natural conservation of interacting sequences. These viruses would be at a selective advantage not only by breaking recessive resistance by hosts but also by extending host range to nonhosts.

FUTURE DIRECTIONS

The studies described here have led to a number of intriguing questions that require further investigation before 3′ CITEs can be fully understood. For instance, many *Tombusviridae* viruses have no sequences or structures that resemble a known CITE. These viruses may contain CITEs that deviate so far from current definitions of consensus as to be unrecognizable, whereas others likely harbor still more classes of CITEs yet to be discovered. A second question is whether a subset of animal viruses and host mRNAs also harbor 3′ elements that through binding to eIF4F/eIF4E/eIF4G or ribosomes can effectively enhance translation. Ribosome binding to the 3′ UTRs of TCV and PEMV2 was investigated only after molecular modeling predicted the presence of internal tRNA-like structures (28). Thus, it remains unknown whether other coding RNAs harbor a combination of secondary structure elements that might likewise assume a three-dimensional T-shaped form that binds ribosomes or ribosomal subunits. Because the structure of 3′ CITEs can provide clues to mechanisms of action, high-resolution structures of CITE(s) interacting with their cognate initiation factor are needed to identify new ways in which eIF4F can be recruited. Finally,

important mechanistic questions remain concerning how known 3′ CITEs deliver ribosomes to the 5′ end of the viral genome. For example, do ribosomes bind to a non-TSS 3′ CITE before or after the CITE base-pairs with its 5′ interacting sequence, and how does the ribosome access the very 5′ end of the RNA? Because it seems unlikely that only plant viruses have evolved such useful 3′ translational enhancers, these future studies will likely reveal additional ways in which mRNAs recruit the translational machinery in the absence of a functional 5 ′ cap or, possibly, enhance cap-dependent translation.

Acknowledgments

This work was supported by grants from the U.S. Public Health Service (GM 061515-05A2/G120CD and GM 061515-07S1 to A.E.S. and 2 R01 GM067104 to W.A.M.) and NSF (MCB 1157906) to A.E.S. The authors thank Nikki Krueger for aligning the sequences and constructing the tree in Figure 6.

Glossary

3′ cap-independent translation enhancer (CITE)	required for efficient translation of plant viruses lacking 3′ caps and usually 3′ poly(A) tails
Internal ribosome entry site (IRES)	an RNA element located at or near the initiation codon in cellular or viral mRNAs that recruits the ribosome either with or without a requirement for initiation factors allowing translation in a cap-independent fashion
TED	translation enhancer domain
Kissing-loop interaction	base-pairing between two nucleic acid hairpin loops that contain partially or fully complementary bases, thereby forming a composite coaxially stacked helix
BTE	*Barley yellow dwarf virus*-like translation element
Non-Watson-Crick interaction	any base-pairing between nucleotides with a geometry different from that described by Watson and Crick
PTE	*Panicum mosaic virus*-like translation enhancer
RNA pseudoknot	a tertiary structure found in a wide variety of RNA and produced when a single-stranded segment pairs with a single-stranded hairpin loop, leading to a structure with at least two helical stems and two loops crossing the grooves of the helices
SHAPE (selective 2′-hydroxyl acylation analyzed by primer extension)	a technique for determining RNA structure that reports on the flexibility of nucleotides
ISS	I-shaped structure
YSS	Y-shaped structure
TSS	T-shaped structure

RdRp	RNA-dependent RNA polymerase
kl-TSS	kissing-loop T-shaped structure
RNA recombination	a process mediated by the viral RdRp or host RNases that results in the addition or replacement of segments of viral RNA

LITERATURE CITED

1. Batten JS, Desvoyes B, Yamamura Y, Scholthof KB. A translational enhancer element on the 3′-proximal end of the *Panicum mosaic virus* genome. FEBS Lett. 2006; 580:2591–97. [PubMed: 16647707]
2. Carpenter CD, Simon AE. In vivo restoration of biologically active 3′ ends of virus-associated RNAs by nonhomologous RNA recombination and replacement of a terminal motif. J Virol. 1996; 70:478–86. [PubMed: 8523561]
3. Chattopadhyay M, Shi K, Yuan X, Simon AE. Long-distance kissing loop interactions between a 3′ proximal Y-shaped structure and apical loops of 5′ hairpins enhance translation of *Saguaro cactus virus*. Virology. 2011; 417:113–25. [PubMed: 21664637]
4. Danthinne X, Seurinck J, Meulewaeter F, Van Montagu M, Cornelissen M. The 3′ untranslated region of satellite tobacco necrosis virus RNA stimulates translation in vitro. Mol Cell Biol. 1993; 13:3340–49. [PubMed: 8497255]
5. Diaz JA, Nieto C, Moriones E, Truniger V, Aranda MA. Molecular characterization of a *Melon necrotic spot virus* strain that overcomes the resistance in melon and nonhost plants. Mol Plant-Microbe Interact. 2004; 17:668–75. [PubMed: 15195949]
6. Dreher TW. Role of tRNA-like structures in controlling plant virus replication. Virus Res. 2009; 139:217–29. [PubMed: 18638511]
7. Dreher TW, Miller WA. Translational control in positive strand RNA plant viruses. Virology. 2006; 344:185–97. [PubMed: 16364749]
8. Fabian MR, White KA. 5′-3′ RNA-RNA interaction facilitates cap- and poly(A) tail-independent translation of Tomato bushy stunt virus mRNA: a potential common mechanism for Tombusviridae. J Biol Chem. 2004; 279:28862–72. [PubMed: 15123633]
9. Fabian MR, White KA. Analysis of a 3′-translation enhancer in a tombusvirus: a dynamic model for RNA-RNA interactions of mRNA termini. RNA. 2006; 12:1304–14. [PubMed: 16682565]
10. Gao F, Kasprzak W, Stupina VA, Shapiro BA, Simon AE. PEMV ribosome-binding 3′ translational enhancer has a T-shaped structure and engages in a long-distance RNA-RNA interaction. J Virol. 2012; 86:9828–42. Identified the first kl-TSS, a ribosome-binding 3′ CITE that can engage in a long-distance kissing-loop interaction. [PubMed: 22761367]
11. Gazo BM, Murphy P, Gatchel JR, Browning KS. A novel interaction of cap-binding protein complexes eukaryotic initiation factor (eIF) 4F and eIF(iso)4F with a region in the 3′-untranslated region of satellite tobacco necrosis virus. J Biol Chem. 2004; 279:13584–92. First demonstration of a translation initiation factor binding to a 3′ CITE. [PubMed: 14729906]
12. Gold L, Brown D, He Y, Shtatland T, Singer BS, Wu Y. From oligonucleotide shapes to genomic SELEX: novel biological regulatory loops. Proc Natl Acad Sci USA. 1997; 94:59–64. [PubMed: 8990161]
13. Guo L, Allen E, Miller WA. Structure and function of a cap-independent translation element that functions in either the 3′ or the 5′ untranslated region. RNA. 2000; 6:1808–20. [PubMed: 11142380]
14. Guo L, Allen E, Miller WA. Base-pairing between untranslated regions facilitates translation of uncapped, nonpolyadenylated viral RNA. Mol Cell. 2001; 7:1103–9. Determined that a long-distance kissing-loop interaction was important for translational enhancement by a 3′ CITE (the BTE). [PubMed: 11389856]

15. Hebrard E, Poulicard N, Gerard C, Traore O, Wu HC, et al. Direct interaction between the *Rice yellow mottle virus* (RYMV) VPg and the central domain of the rice eIF(iso)4G1 factor correlates with rice susceptibility and RYMV virulence. Mol Plant-Microbe Interact. 2010; 23:1506–13. [PubMed: 20653414]
16. Heus HA, Pardi A. Structural features that give rise to the unusual stability of RNA hairpins containing GNRA loops. Science. 1991; 253:191–94. [PubMed: 1712983]
17. Ishibashi K, Naito S, Meshi T, Ishikawa M. An inhibitory interaction between viral and cellular proteins underlies the resistance of tomato to nonadapted tobamoviruses. Proc Natl Acad Sci USA. 2009; 106:8778–83. [PubMed: 19423673]
18. Jackson RJ, Hellen CU, Pestova TV. The mechanism of eukaryotic translation initiation and principles of its regulation. Nat Rev Mol Cell Biol. 2010; 11:113–27. [PubMed: 20094052]
19. Jiang Y, Cheng CP, Serviene E, Shapka N, Nagy PD. Repair of lost 5′ terminal sequences in tombusviruses: rapid recovery of promoter- and enhancer-like sequences in recombinant RNAs. Virology. 2010; 404:96–105. [PubMed: 20537671]
20. Karetnikov A, Keranen M, Lehto K. Role of the RNA2 3′ non-translated region of *Blackcurrant reversion nepovirus* in translational regulation. Virology. 2006; 354:178–91. [PubMed: 16876845]
21. Karetnikov A, Lehto K. The RNA2 5′ leader of *Blackcurrant reversion virus* mediates efficient in vivo translation through an internal ribosomal entry site mechanism. J Gen Virol. 2007; 88:286–97. [PubMed: 17170462]
22. Karetnikov A, Lehto K. Translation mechanisms involving long-distance base pairing interactions between the 5′ and 3′ non-translated regions and internal ribosomal entry are conserved for both genomic RNAs of *Blackcurrant reversion nepovirus*. Virology. 2008; 371:292–308. [PubMed: 17976678]
23. Kneller ELP, Rakotondrafara AM, Miller WA. Cap-independent translation of plant viral RNAs. Virus Res. 2006; 119:63–75. [PubMed: 16360925]
24. Kraft JJ, Treder K, Peterson MS, Miller WA. Cation-dependent folding of cap-independent translation elements facilitates interaction of a 17 nucleotide conserved sequence with eIF4G. Nucleic Acids Res. 2013; 41:3398–413. [PubMed: 23361463]
25. Legault P, Li J, Mogridge J, Kay LE, Greenblatt J. NMR structure of the bacteriophage λN peptide/*boxB* RNA complex: recognition of a GNRA fold by an arginine-rich motif. Cell. 1998; 93:289–99. [PubMed: 9568720]
26. Marcotrigiano J, Lomakin IB, Sonenberg N, Pestova TV, Hellen CU, Burley SK. A conserved HEAT domain within eIF4G directs assembly of the translation initiation machinery. Mol Cell. 2001; 7:193–203. [PubMed: 11172724]
27. Martin F, Barends S, Jaeger S, Schaeffer L, Prongidi-Fix L, Eriani G. Cap-assisted internal initiation of translation of histone H4. Mol Cell. 2011; 41:197–209. [PubMed: 21255730]
28. McCormack JC, Yuan X, Yingling YG, Kasprzak W, Zamora RE, et al. Structural domains within the 3′ untranslated region of *Turnip crinkle virus*. J Virol. 2008; 82:8706–20. First demonstration that T-shaped structures form in an internal position in the 3 ′ UTR of a viral RNA. [PubMed: 18579599]
29. Meulewaeter F, Danthinne X, Van Montagu M, Cornelissen M. 5′- and 3′-sequences of satellite tobacco necrosis virus RNA promoting translation in tobacco. Plant J. 1998; 14:169–76. [PubMed: 9628014]
30. Meulewaeter F, van Lipzig R, Gultyaev AP, Pleij CW, Van Damme D, et al. Conservation of RNA structures enables TNV and BYDV 5′ and 3′ elements to cooperate synergistically in cap-independent translation. Nucleic Acids Res. 2004; 32:1721–30. [PubMed: 15020708]
31. Mizumoto H, Tatsuta M, Kaido M, Mise K, Okuno T. Cap-independent translational enhancement by the 3′ untranslated region of *Red clover necrotic mosaic virus RNA1*. J Virol. 2003; 77:12113–21. [PubMed: 14581548]
32. Moury B, Morel C, Johansen E, Guilbaud L, Souche S, et al. Mutations in *Potato virus Y* genome-linked protein determine virulence toward recessive resistances in *Capsicum annuum* and *Lycopersicon hirsutum*. Mol Plant-Microbe Interact. 2004; 17:322–29. [PubMed: 15000399]
33. Nicholson BL, White KA. 3′ Cap-independent translation enhancers of positive-strand RNA plant viruses. Curr Opin Virol. 2011; 1:373–80. [PubMed: 22440838]

34. Nicholson BL, Wu B, Chevtchenko I, White KA. Tombusvirus recruitment of host translational machinery via the 3′ UTR. RNA. 2010; 16:1402–19. Showed that the ISS 3′ CITE can simultaneously bind to eIF4F and the 5′ UTR and that this complex is required for recruiting ribosomes to the 5′ end of the viral RNA genome. [PubMed: 20507975]
35. Nicholson BL, Zaslaver O, Mayberry LK, Browning KS, White KA. Tombusvirus Y-shaped translational enhancer forms a complex with eIF4F and can be functionally replaced by heterologous translational enhancers. J Virol. 2013; 87:1872–83. Demonstrated binding of the CIRV YSS to eIF4F and eIFiso4F and that YSS can be functionally replaced by the PTE or ISS 3′ CITE. [PubMed: 23192876]
36. Niedzwiecka A, Marcotrigiano J, Stepinski J, Jankowska-Anyszka M, Wyslouch-Cieszynska A, et al. Biophysical studies of eIF4E cap-binding protein: recognition of mRNA 5′ cap structure and synthetic fragments of eIF4G and 4E-BP1 proteins. J Mol Biol. 2002; 319:615–35. [PubMed: 12054859]
37. Nieto C, Morales M, Orjeda G, Clepet C, Monfort A, et al. An eIF4E allele confers resistance to an uncapped and non-polyadenylated RNA virus in melon. Plant J. 2006; 48:452–62. [PubMed: 17026540]
38. Nieto C, Rodriguez-Moreno L, Rodriguez-Hernandez AM, Aranda MA, Truniger V. *Nicotiana benthamiana* resistance to non-adapted *Melon necrotic spot virus* results from an incompatible interaction between virus RNA and translation initiation factor 4E. Plant J. 2011; 66:492–501. [PubMed: 21255163]
39. Pallas V, Antonio Garcia J. How do plant viruses induce disease? Interactions and interference with host components. J Gen Virol. 2011; 92:2691–705. [PubMed: 21900418]
40. Paranjape SM, Harris E. Control of dengue virus translation and replication. Curr Top Microbiol Immunol. 2010; 338:15–34. [PubMed: 19802575]
41. Patrick RM, Browning KS. The eIF4F and eIFiso4F complexes of plants: an evolutionary perspective. Comp Funct Genomics. 2012; 2012:287814. [PubMed: 22611336]
42. Perez K, Yeam I, Kang B-C, Ripoll DR, Kim J, et al. *Tobacco etch virus* infectivity in *Capsicum* spp. is determined by a maximum of three amino acids in the viral virulence determinant VPg. Mol Plant-Microbe Interact. 2012; 25:1562–73. [PubMed: 23134519]
43. Prevot D, Decimo D, Herbreteau CH, Roux F, Garin J, et al. Characterization of a novel RNA-binding region of eIF4GI critical for ribosomal scanning. EMBO J. 2003; 22:1909–21. [PubMed: 12682023]
44. Rakotondrafara AM, Polacek C, Harris E, Miller WA. Oscillating kissing stem-loop interactions mediate 5′ scanning-dependent translation by a viral 3′-cap-independent translation element. RNA. 2006; 12:1893–906. [PubMed: 16921068]
45. Reinbold C, Lacombe S, Ziegler-Graff V, Scheidecker D, Wiss L, et al. Closely related poleroviruses depend on distinct translation initiation factors to infect *Arabidopsis thaliana*. Mol Plant-Microbe Interact. 2013; 26:257–65. [PubMed: 23013438]
46. Reineke LC, Lloyd RE. Animal virus schemes for translation dominance. Curr Opin Virol. 2011; 1:363–72. [PubMed: 22319551]
47. Robaglia C, Caranta C. Translation initiation factors: a weak link in plant RNA virus infection. Trends Plant Sci. 2006; 11:40–45. [PubMed: 16343979]
48. Ruffel S, Dussault MH, Palloix A, Moury B, Bendahmane A, et al. A natural recessive resistance gene against potato virus Y in pepper corresponds to the eukaryotic initiation factor 4E (eIF4E). Plant J. 2002; 32:1067–75. [PubMed: 12492847]
49. Sarawaneeyaruk S, Iwakawa H-O, Mizumoto H, Murakami H, Kaido M, et al. Host-dependent roles of the viral 5′ untranslated region (UTR) in RNA stabilization and cap-independent translational enhancement mediated by the 3′ UTR of *Red clover necrotic mosaic virus* RNA1. Virology. 2009; 391:107–18. [PubMed: 19577782]
50. Scheets K, Redinbaugh MG. Infectious cDNA transcripts of *Maize necrotic streak virus*: infectivity and translational characteristics. Virology. 2006; 350:171–83. [PubMed: 16545417]
51. Schmeing TM, Ramakrishnan V. What recent ribosome structures have revealed about the mechanism of translation. Nature. 2009; 461:1234–42. [PubMed: 19838167]

52. Shen R, Miller WA. The 3′ untranslated region of tobacco necrosis virus RNA contains a barley yellow dwarf virus-like cap-independent translation element. J Virol. 2004; 78:4655–64. [PubMed: 15078948]
53. Song YT, Friebe P, Tzima E, Junemann C, Bartenschlager R, Niepmann M. The hepatitis C virus RNA 3′-untranslated region strongly enhances translation directed by the internal ribosome entry site. J Virol. 2006; 80:11579–88. [PubMed: 16971433]
54. Stupina VA, Meskauskas A, McCormack JC, Yingling YG, Shapiro BA, et al. The 3′ proximal translational enhancer of *Turnip crinkle virus* binds to 60S ribosomal subunits. RNA. 2008; 14:2379–93. First demonstration that ribosomes can bind to 3′ CITEs and that binding is important for translational enhancement. [PubMed: 18824512]
55. Stupina VA, Yuan X, Meskauskas A, Dinman JD, Simon AE. Ribosome binding to a 5′ translational enhancer is altered in the presence of the 3′ UTR in cap-independent translation of *Turnip crinkle virus*. J Virol. 2011; 85:4638–53. [PubMed: 21389125]
56. Timmer RT, Benkowski LA, Schodin D, Lax SR, Metz AM, et al. The 5′ and 3′ untranslated regions of satellite tobacco necrosis virus RNA affect translational efficiency and dependence on a 5′ cap structure. J Biol Chem. 1993; 268:9504–10. [PubMed: 8486640]
57. Treder K, Pettit Kneller EL, Allen EM, Wang Z, Browning KS, Miller WA. The 3′ cap-independent translation element of *Barley yellow dwarf virus* binds eIF4F via the eIF4G subunit to initiate translation. RNA. 2008; 14:134–47. [PubMed: 18025255]
58. Truniger V, Nieto C, Gonzalez-Ibeas D, Aranda M. Mechanism of plant eIF4E-mediated resistance against a carmovirus (*Tombusviridae*): cap-independent translation of a viral RNA controlled in *cis* by an (a)virulence determinant. Plant J. 2008; 56:716–27. Showed that differences in the ISS 3′ CITE of MNSV were responsible for overcoming recessive resistance that mapped to eIF4E. [PubMed: 18643998]
59. van Lipzig R, Gultyaev AP, Pleij CW, van Montagu M, Cornelissen M, Meulewaeter F. The 5′ and 3′ extremities of the satellite tobacco necrosis virus translational enhancer domain contribute differentially to stimulation of translation. RNA. 2002; 8:229–36. [PubMed: 11924567]
60. Wang A, Krishnaswamy S. Eukaryotic translation initiation factor 4E-mediated recessive resistance to plant viruses and its utility in crop improvement. Mol Plant Pathol. 2012; 13:795–803. [PubMed: 22379950]
61. Wang M-B, Masuta C, Smith NA, Shimura H. RNA silencing and plant viral diseases. Mol Plant-Microbe Interact. 2012; 25:1275–85. [PubMed: 22670757]
62. Wang S, Browning KS, Miller WA. A viral sequence in the 3′-untranslated region mimics a 5′ cap in facilitating translation of uncapped mRNA. EMBO J. 1997; 16:4107–16. [PubMed: 9233819]
63. Wang S, Miller WA. A sequence located 4.5 to 5 kilobases from the 5′ end of the barley yellow dwarf virus (PAV) genome strongly stimulates translation of uncapped mRNA. J Biol Chem. 1995; 270:13446–52. [PubMed: 7768947]
64. Wang Z, Kraft JJ, Hui AY, Miller WA. Structural plasticity of *Barley yellow dwarf virus*-like cap-independent translation elements in four genera of plant viral RNAs. Virology. 2010; 402:177–86. [PubMed: 20392470]
65. Wang Z, Parisien M, Scheets K, Miller WA. The cap-binding translation initiation factor, eIF4E, binds a pseudoknot in a viral cap-independent translation element. Structure. 2011; 19:868–80. First analysis of how a 3′ CITE (PEMV2 PTE) interacts with a bound translation initiation factor, leading to a new mechanism for mRNA recognition by elF4E. [PubMed: 21645857]
66. Wang Z, Treder K, Miller WA. Structure of a viral cap-independent translation element that functions via high affinity binding to the eIF4E subunit of eIF4F. J Biol Chem. 2009; 284:14189–202. [PubMed: 19276085]
67. White KA, Nagy PD. Advances in the molecular biology of tombusviruses: gene expression, genome replication, and recombination. Prog Nucleic Acids Res Mol Biol. 2004; 78:187–226.
68. Yoshii M, Nishikiori M, Tomita K, Yoshioka N, Kozuka R, et al. The *Arabidopsis cucumovirus* multiplication 1 and 2 loci encode translation initiation factors 4E and 4G. J Virol. 2004; 78:6102–11. [PubMed: 15163703]

69. Yoshii M, Yoshioka N, Ishikawa M, Naito S. Isolation of an *Arabidopsis thaliana* mutant in which the multiplication of both cucumber mosaic virus and turnip crinkle virus is affected. J Virol. 1998; 72:8731–37. [PubMed: 9765416]

70. Yuan XF, Shi KR, Meskauskas A, Simon AE. The 3′ end of *Turnip crinkle virus* contains a highly interactive structure including a translational enhancer that is disrupted by binding to the RNA-dependent RNA polymerase. RNA. 2009; 15:1849–64. [PubMed: 19656866]

71. Yuan XF, Shi KR, Simon AE. A local, interactive network of 3′ RNA elements supports translation and replication of *Turnip crinkle virus*. J Virol. 2012; 86:4065–81. [PubMed: 22345459]

72. Yuan XF, Shi KR, Young MYL, Simon AE. The terminal loop of a 3′ proximal hairpin plays a critical role in replication and the structure of the 3′ region of *Turnip crinkle virus*. Virology. 2010; 402:271–80. [PubMed: 20403628]

73. Zhang GH, Zhang JC, Simon AE. Repression and derepression of minus-strand synthesis in a plus-strand RNA virus replicon. J Virol. 2004; 78:7619–33. [PubMed: 15220437]

74. Zuo XB, Wang JB, Yu P, Eyler D, Xu H, et al. Solution structure of the cap-independent translational enhancer and ribosome-binding element in the 3′ UTR of *Turnip crinkle virus*. Proc Natl Acad Sci USA. 2010; 107:1385–90. Confirmed the structure of the TCV TSS as a tRNA-like element by a novel NMR-SAXS protocol. [PubMed: 20080629]

SUMMARY POINTS

1. Most (if not all) plant RNA viruses without 5′ caps and 3′ poly(A) tails contain at least one CITE in their 3′ UTR that enhances translation through binding to either translation initiation factors (eIF4E, eIF4G, eIF4F) or ribosomes and ribosomal subunits.
2. 3′ CITEs have secondary structures that are I-shaped, Y-shaped, and T-shaped, or that have helical spokes radiating from a central hub. For the BTE, which contains the helical spokes, interaction with eIF4G involves sequences in a highly conserved BTE helix and sequences in the hub near the proximal ends of one or more additional helices.
3. Nearly all 3′ CITEs are associated with a known or predicted long-distance kissing-loop interaction with a 5′ hairpin that is located either in the 5′ UTR or in the nearby coding region. The interacting sequences for 3′ CITEs of carmoviruses as well as other viruses are conserved (YGCCA/UGGCR), with either sequence appearing at either end of the virus.
4. The TCV and PEMV2 TSS differ in their ribosomal subunit binding properties and their binding location within the ribosome. 3′ bound ribosomes and ribosomal subunits bound to the kl-TSS may be transferred to the 5′ end via a compatible long-distance RNA-RNA interaction involving a kl-TSS hairpin loop in a reaction that may mimic a codon-anticodon interaction. 60S subunits bound to the TCV TSS may join 40S subunits interacting at the 5′ end to circularize the viral genome.
5. Some 3′ CITEs are interchangeable, as long as the long-distance RNA-RNA interaction is maintained. In infectious genomic clones, one type of CITE can be replaced with another type to yield infectious virus. Evidence exists for natural exchange of CITEs, as the distribution of 3′ CITEs among viruses does not correlate with taxonomic relationships. Moreover, natural recombination in MNSV replaced one 3′ CITE with a different CITE from an unidentified virus, allowing the virus to break host resistance. These observations reveal the modular evolution of these elements.
6. Nearly all natural recessive genetic resistance involves changes in host translation initiation factors. In some cases this change prevents interaction with a particular virus CITE, making acquisition of a new functional CITE an effective way of bypassing host resistance and extending host range.

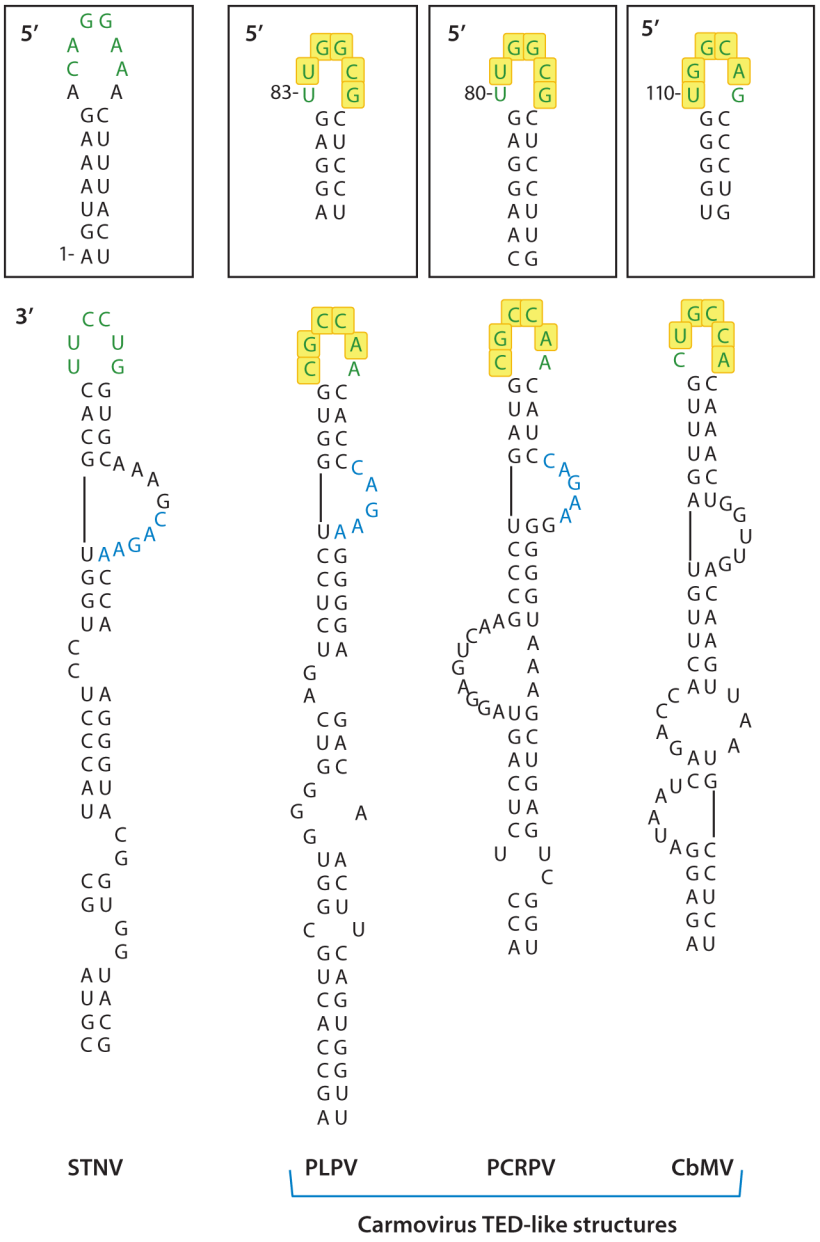

Figure 1.

Predicted structure of the STNV TED. Sequences involved in putative long-distance RNA-RNA interaction with 5′ sequences (*boxed*) are in green. Yellow boxes denote the conserved interacting sequences found in carmovirus TED-like, ISS, and PTE class CITEs. Sequences in blue are conserved between the STNV TED and the PLPV and PCRPV TED-like structures. Numbering is from the 5′ end of the viral genome. Abbreviations: CITE, cap-independent translational enhancer; CbMV, *Calibrachoa mottle virus*; ISS, I-shaped structure; PLPV, *Pelargonium line pattern virus*; PCRPV, *Pelargonium chlorotic ring pattern virus*; PTE, *Panicum mosaic virus*-like translational enhancer; STNV, *Satellite tobacco necrosis virus*; TED, translation enhancer domain.

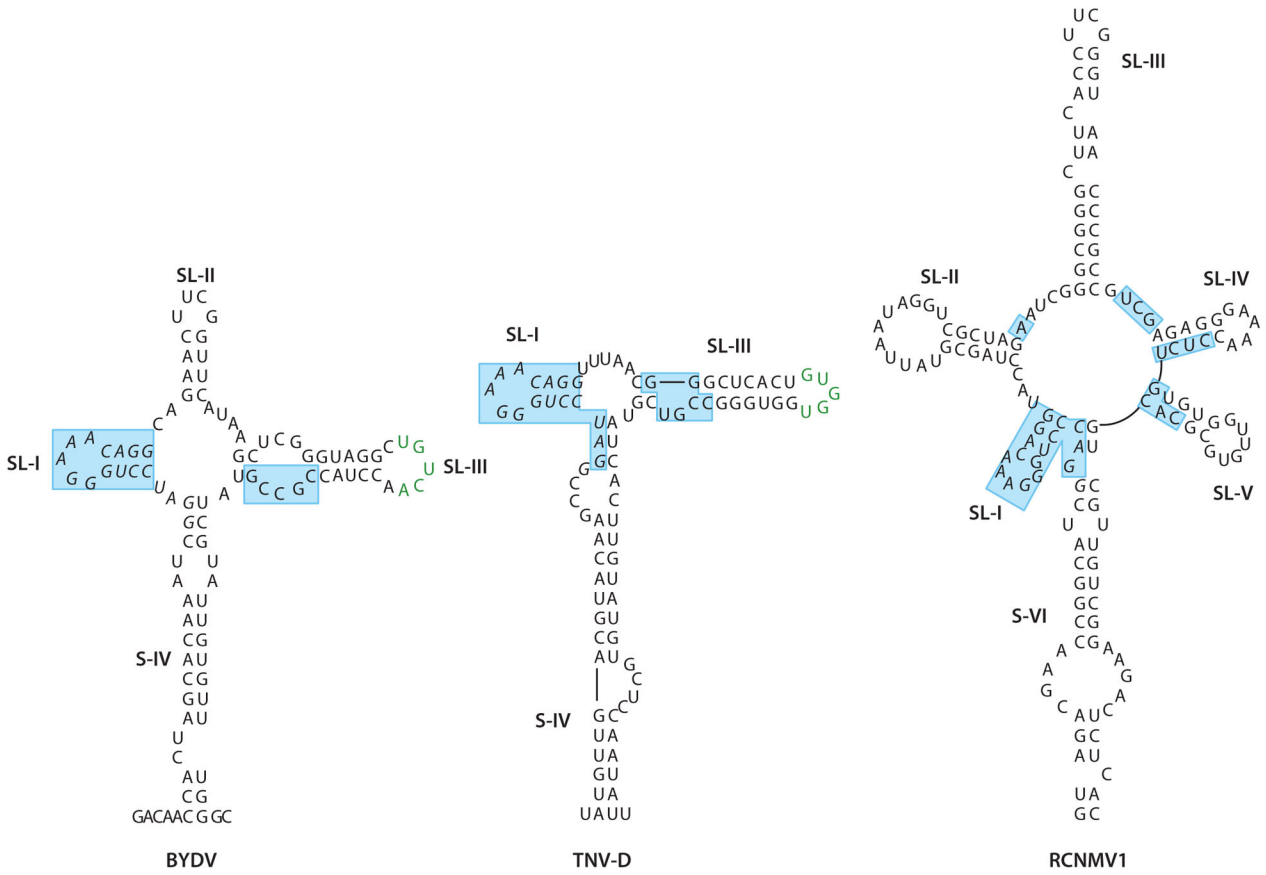

Figure 2.

Secondary structures of representative BTEs from the *Luteovirus* (BYDV), *Necrovirus* (TNV-D), and *Dianthovirus* (RCNMV1) genera. Stem (S) or stem loop (SL) numbers are indicated. The 17-nucleotide conserved sequence is in italics. Regions shaded in blue are protected from chemical modification by a functional truncation of eIF4G, indicating the likely eIF4G-binding site (24). Note that this includes most of the 17-nucleotide conserved sequence and other bases around the central hub. Green bases pair with the 5′ UTR for efficient translation. Loops in RCNMV1 BTE complement bases in the 5′ UTR, but this complementarity is not necessary for efficient translation (49). This figure is modified and reprinted with permission from Reference 24. Abbreviations: BTE, *Barley yellow dwarf virus*-like element; BYDV, *Barley yellow dwarf virus*; RCNMV1, *Red clover necrotic mosaic virus RNA1*; TNV-D, *Tobacco necrosis virus*-D; UTR, untranslated region.

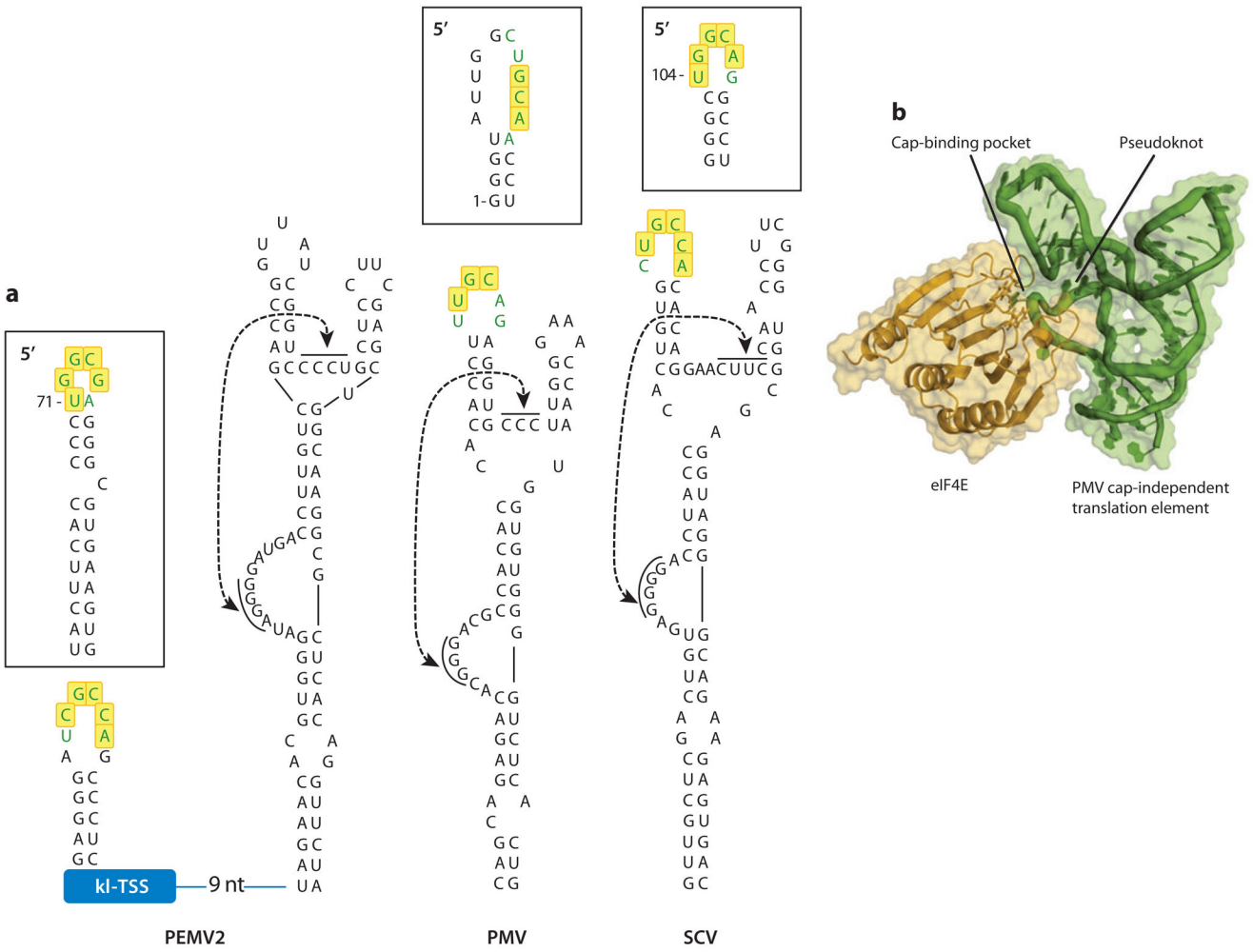

Figure 3.

Structures of three PTEs. (*a*) Representative PTE structures found in viruses in different genera (*Umbravirus*, PEMV2; *Panicovirus*, PMV; *Carmovirus*, SCV). Sequences involved in putative long-distance RNA-RNA interaction with 5′ sequences (*boxed*) are in green typeface. Yellow boxes denote the conserved interacting sequences found in carmovirus TED-like, ISS, and PTE class CITEs. The PEMV2 PTE has no interacting sequence but instead uses the interacting sequence of the adjacent kl-TSS 3′ CITE (see Figure 5***b,c*** for the structure of this CITE). Potential pseudoknots are indicated by the double-headed arrow. Numbering is from the 5′ end of the viral genome. (*b*) Model of eIF4E docked to the PEMV PTE. This model is consistent with structure-probing and footprinting data. Reprinted from Reference 65 with permission. Abbreviations: kl-TSS, kissing-loop T-shaped structure; PEMV2, *Pea enation mosaic virus RNA 2*; PMV, *Panicum mosaic virus*; PTE, *Panicum mosaic virus*-like translational enhancer; SCV, *Saguaro cactus virus*; TED, translation enhancer domain; ISS, I-shaped structure; CITE, cap-independent translational enhancer.

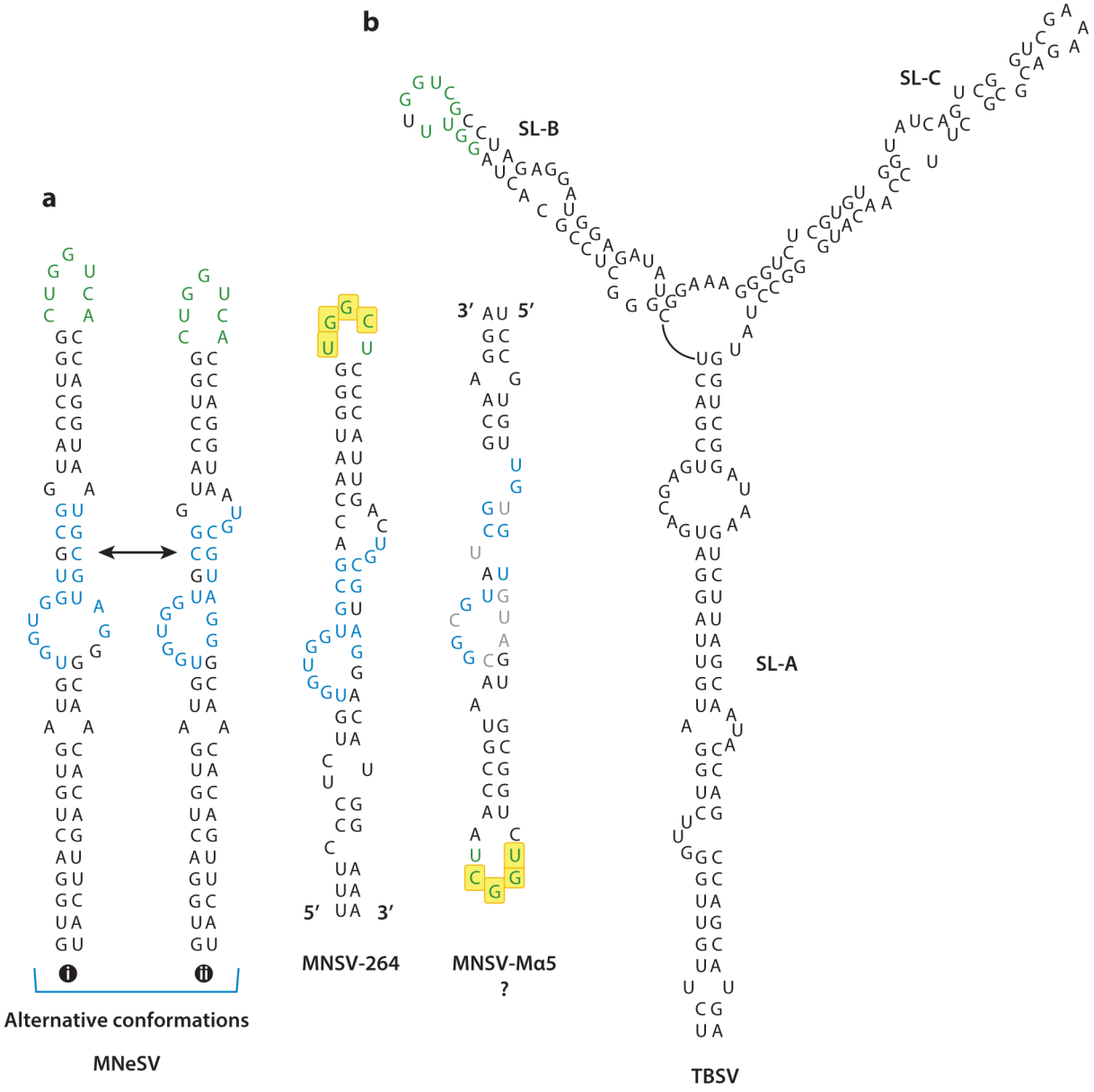

Figure 4.

ISS and YSS secondary structures. Bases in green typeface pair with sequences in the 5′ UTR. (*a*) Alternative secondary structures of the MNeSV ISS. Structure *i* was predicted by Mfold and was supported, in part, by chemical probing and mutagenesis (34). Structure *ii* is the predicted structure of the MNeSV ISS selected in a chimeric replicating virus consisting of *Carnation Italian ringspot virus* containing an ISS in place of a YSS translational enhancer (35). All five known ISS, except for the MNSV-M*α*5 ISS, can form both structures. MNSV-M*α*5 can form a similar structure in an inverted orientation (*right*). Bases in blue typeface are conserved in all but the MNSV-M*α*5 ISS, and mutation of these bases in the MNeSV ISS reduces its function (36, 37). Bases in gray typeface are those in the inverted MNSV-M*α*5 ISS that defy the consensus. Bases in yellow boxes contain the

conserved carmovirus interaction sequence. (*b*) Secondary structure of the TBSV YSS, supported by chemical probing and mutagenesis (8). Abbreviations: ISS, I-shaped structure; MNeSV, *Maize necrotic streak virus*; MNSV, *Melon necrotic spot virus*; TBSV, *Tomato bushy stunt virus*; UTR, untranslated region; YSS, Y-shaped structure.

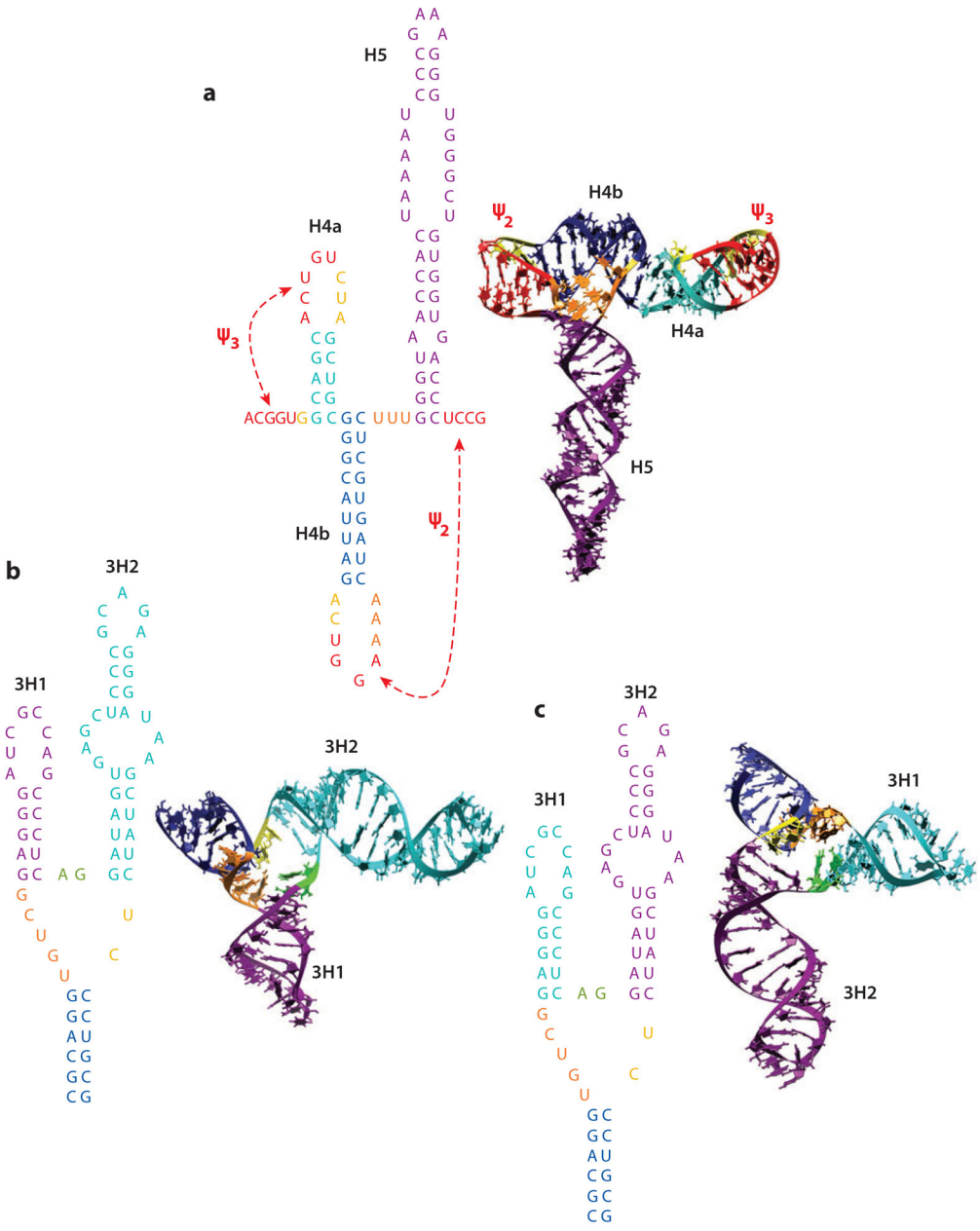

Figure 5.

Two-dimensional and three-dimensional structures of the TCV TSS and PEMV kl-TSS. (*a*) The TCV TSS, composed of three hairpins and two pseudoknots. No long-distance interaction is discernible for the TCV TSS or nearby sequences (55). (*b*, *c*) Two possible configurations of the PEMV kl-TSS. The loop of kl-TSS hairpin 3H1 engages in an RNA-RNA interaction with a 5′ coding sequence hairpin (see Figure 3a), which is compatible with simultaneous ribosome binding (F. Gao & A.E. Simon, unpublished data). (*b*) Hairpin 3H1 mimics a short anticodon stem. (*c*) Hairpin 3H2 occupies the anticodon stem position. The TCV TSS binds to 60S and 80S ribosomes (54), whereas the PEMV kl-TSS binds to 40S, 60S, and 80S ribosomes (10). The TCV TSS and PEMV kl-TSS do not compete with each

other for binding to plant 80S ribosomes (F. Gao & A.E. Simon, unpublished data). Three-dimensional structures courtesy of B. Shapiro & W. Kasprzak (National Cancer Institute). Abbreviations: kl, kissing loop; PEMV, *Pea enation mosaic virus*; TCV, *Turnip crinkle virus*; TSS, T-shaped structure.

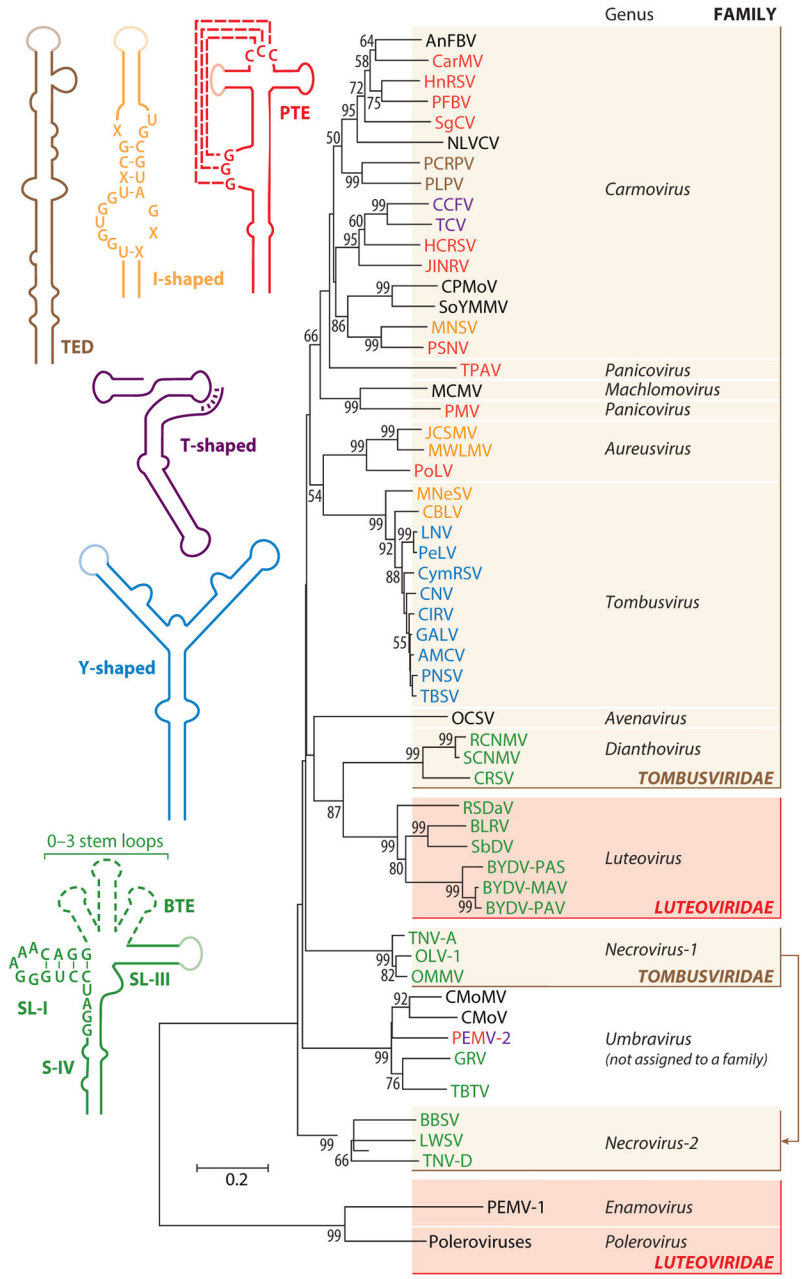

Figure 6.

Phylogenetic tree of selected *Tombusviridae* and *Tombusviridae*-related viruses based on RdRp sequences. Virus acronyms are color-coded to match the type of 3′ CITE (two-dimensional structure at left) they contain. Lighter-shaded loops in the secondary structure diagrams indicate sequences known or predicted to base-pair to the 5′ end of the viral RNA. CITEs have not been identified for viruses in black typeface. RdRp sequences were aligned using the Muscle multiple sequence alignment algorithm and optimized using JalView version 2.6.1. Trees were generated from the alignment using MEGA5 via the neighbor-joining method and 1,000 replicates for the bootstrap. The authors thank Nikki Krueger for constructing the tree. Abbreviations: RdRp, RNA-dependent RNA polymerase; CITE, cap-

independent translational enhancer; TED, translation enhancer domain; PTE, *Panicum mosaic virus*-like translational enhancer; BTE, *Barley yellow dwarf virus*-like element; S, stem; SL, stem loop.

Table 1

Virus	CITE Type	3′ CITE sequence[a]	5′ hairpin sequence[a]	5′ hairpin location
		Carmovirus		
SCV	PTE	CUGCCA	UGGCAG	5′ ORF
PFBV	PTE	CUGCCA	UGGCAG	5′ ORF
CarMV	PTE	CUGCCA	UGGCGG	5′ terminus
HnRSV	PTE	CUGCCA	UGGCAG	5′ ORF
HCRSV	PTE	GCCA	UGGC	5′ terminus
GaMV	PTE	UUGGCG	CGCCAA	5′ terminus
PSNV	PTE	UUGGCG	GCCA	5′ UTR
MNSV	ISS	UGGCU	AGCCA	5′ ORF
TGP-carmo	ISS	CGGCAA	UUGCCG	5′ terminus
CbMV	TED-like	CUGCCA	UGGCAG	5′ ORF
PLPV	TED-like	CGCCAA	UUGGCG	5′ ORF
PCRPV	TED-like	CGCCAA	UUGGCG	5′ ORF
		Umbravirus		
PEMV	kl-TSS	UCGCCA	UGGCGA	5′ ORF
		Panicovirus		
PMV	PTE	UUGCAG	CUGCAA	5′ terminus
CMMV	PTE	UUGCCG	CGGCAA	5′ terminus
		Necrovirus		
STNV	TED	UUCCUG	CAGGAA	5′ terminus
TNV-D	BTE	UGGU	ACCA	5′ terminus
OLV-1	BTE	UGGUG	UACCA	5′ terminus
LWSV	BTE	UGGU	ACCA	5′ terminus
		Tombusvirus		
TBSV	YSS	GGUCG	CGACC	5′ UTR
MNeSV	ISS	UGGUCA	UGACCG	5′ UTR
		Luteovirus		

Virus	CITE Type	3′ CITE sequence[a]	5′ hairpin sequence[a]	5′ hairpin location
BYDV genome	BTE	UGUCA	UGACA	4th SL of 5′ UTR
BYDV sgRNA1	BTE	UGUCA	UGACA	5′ terminus
SbDV	BTE	UGUCA	UGACA	5′ terminus
RSDaV	BTE	UGUCA	UGACA	5′ terminus

[a]Conserved interacting sequences (YGCCA/UGGCR) are in red and orange.

Note that either sequence can be in the 5′ or 3′ elements.

Abbreviations: SCV, *Saguaro cactus virus;* PFBV, *Pelargonium 3ower break virus;* CarMV, *Carnation mottle virus;* HnRSV, *Honeysuckle ringspot virus;* HCRSV, *Hibiscus chlorotic ringspot virus;* GaMV, *Galinsoga mosaic virus;* PSNV, *Pea stem necrosis virus;* MNSV, *Melon necrotic spot virus;* CbMV, *Calibrachoa mottle virus;* PLPV, *Pelargonium line pattern virus;* PCRPV, *Pelargonium chlorotic ring pattern virus;* PEMV, *Pea enation mosaic virus;* PMV, *Panicum mosaic virus;* CMMV, *Cocksfoot mild mosaic virus;* STNV, *Satellite tobacco necrosis virus;* TNV-D, *Tobacco necrosis virus-D;* OLV-1, *Olive latent virus-1;* LWSV, *Leek white stripe virus;* TBSV, *Tomato bushy stunt virus.*